International Journal of Smart Energy Technology and Environmental Engineering
Volume 2, Issue 1, March 2023
http://globalpublisher.org/journals-1007/

The Impact of a CPVT Polygeneration System on a Home's Energy Bill and Budget

Majid Khazali [1,*]
1- PhD candidate, Department of Industry and Energy, Science and Research Branch, Islamic Azad University, Tehran, Iran
*Corresponding Author: majidkhazali.srbiau@gmail.com

ABSTRACT
The purpose of this research is to investigate the impact, both financially and in terms of energy consumption, of installing a solar-powered photovoltaic thermal concentration (CPVT) system in a residence in Tehran, Iran, so that the homeowner may have access to hot water and air conditioning. Triple-junction solar cells and linear Fresnel concentrators (also known as LFCs) are used in the CPVT system. A water ammonium absorption chiller with a capacity of 5 kilowatts is used so that sun thermal energy may be used to generate cooling electricity. The EES is used to combine the simulation models for both the absorption chiller and the LFC. In the event that solar energy is not adequate, other heaters are now being investigation. In the case that there is an oversupply of solar electricity, the solution that has been proposed makes use of thermal energy storage (TES) tanks. In this configuration, we investigate the possibility of using both conventional photovoltaic cells and concentrated thermal collectors. Furthermore, we investigate the possibility of employing photovoltaic tandem technology (PVT) with both triple-junction and conventional solar cells. Transient simulations of these kinds of systems may be carried out with the help of TRNSYSY. The system that is being suggested produces 5.58 MWh of power, which is enough to satisfy 48% of the building's requirements for energy consumption. The design that has been presented is the one that will save the most money out of the three possible solar systems. The levelized cost of energy is $0.018 USD per kilowatt-hour (kWh), and the benefit-to-cost ratio is 159%. These numbers may be found in the table below. Even though the initial expenditure for a parallel arrangement of two CPVT is only 42% more, the return on investment (ROI) is just 1% worse than it would be otherwise. The very low cost of energy provided by the system is the primary contributor to the payback period's length of 7.8 years.

Keywords: Renewable energy, Trigeneration, Concentrating photovoltaic thermal, Economic evaluation, Single-effect absorption chiller.

1. INTRODUCTION

Shortly after the industrial revolution, the world's energy consumption pattern changed dramatically [1]. Before the industrial revolution, there was a balance between energy production on the earth and energy consumption; the produced plant photosynthesis energy was utilized or stored as coal directly or as oil indirectly. After industrialization, humanity changed the balance by using the past stored energy more than it could be replaced. Although not too long after this, scientists called coal and oil sources of energy non-renewable energy sources. However, waterwheels and windmills were the first types of renewable energy that provided mechanical energy. Still, William Grylls Adams presented the selenium cells' ability to generate electricity as the first modern world method of renewable energy production in 1876 [2]. Soon after, other renewable energy sources are utilized for energy production. But the initial cost of these systems cast them aside until the evidence supporting the Svante Arrhenius's hypothesis that "human activity, carbon dioxide imitations will cause global warming." Surfaced [3]. In contrast to other alternative energy sources, solar energy is available in the majority of locations.

Two primary methods for energy generation from solar energy are solar thermal and solar electrical (PV) collectors. Due to its low cust equipment and high performance solar thermal collectors compared to PV collectors, solar thermal energy production is more compelling [4]. To further improve the cost-efficiency of this system, concentrating units are added. The concentrating solar thermal collectors provide higher temperatures and cost less than the conventional system. Quaschning investigated economic and technical effects of concentrating solar thermal electricity generation compared to the PV system; the results indicate 17% higher power production of the concentrating solar thermal system [5]. The other proposed method to improve solar system efficiency is to combine PV and thermal collectors (PVT). The available energy in this system is a mixture of electrical and thermal energy [6]. Photovoltaic cell efficiency is the function of solar radiation and cell temperature; as a result, reducing cell temperature by extracting the thermal energy of the PVT system results in an improvement in electrical efficiency [7]. To take advantage of both concentrating and PVT systems adopted to a singular structure, CPVT, which in addition to providing electrical and high-quality electrical energy, has a lower cost due to the reduction of the absorber plate of the collector [8]. The high quality of thermal energy in a CPVT system translates to higher cell temperature and lower electrical efficiency. Triple-junction solar cell with a low-efficiency dependence on temperature is a suitable choice for CPVT systems [9].

Owing to the high quality of thermal energy produced by CPVT structures, this structure may be used to power a broad variety of applications. The fundamental idea behind the CPVT is that it can produce both thermal and electrical energy, but it can produce hydrogen, cooling, drying, etc. Mittelman et al. studied single effect absorption combined with a CPVT for cooling. According to the findings of this investigation, the electricity provided by CPVT for the cooling system operates similarly on certain occasions and is even superior to the traditional approach from an economic perspective. [10]. In yet another investigation that was conducted by Mittelman et al. a water desalination system powered by CPVT is

evaluated. The outlines of this research present that the CPVT system has absolute superiority over other types of solar systems for this distillation system and can be, in some cases, more cost-efficient than conventional systems [11]. Buonomano et al. simulate a building's integrated ventilation, heating, and air-conditioning technology for use near Italy. The proposed design for this simulation is a series of PVT and concentrating solar thermal powering single-stage LiBr–H2O absorption chillers. This study finding presents the proposed structure provides more than sufficient energy to meet the building energy demands [12]. Horvat et al. studied working conditions for a solar-powered trigeneration system adopted to provide residential buildings. The results of this study pointed out that utilization of this system could reduce grad dependency of the building located in European[13]. Deymi-Dashtebayaz et al. performed research into the solar photovoltaic thermal mechanism modeling that included a concentrator in addition to a heat pump. The site of the experiment is Mashhad, Iran, and laboratory data are used to confirm the modeling findings. According to this research, when the nanofluid flow rate rises, the solar panel's temperature and the output fluid fall, boosting the thermal and electrical productivity and decreasing the system's exergy efficiency. [14]. Another examination of the thermo-economic improvement of the trigeneration system has been done by Calise et al. In their proposed system, solar, biomass, and geothermal energy are used to supply energy to the system. The products of this structure are heating, cooling, and electricity. This analysis also uses an organic Rankine cycle to generate electricity. This research has been done using TRNSYS software. The location of the study is Naples in southern Italy. The authors state that such a system would result in 139% energy savings, which would result in more energy being produced than needed and a payback period of 19 years [15]. A novel layout for the framework of a heat pump that is driven by a solar photovoltaic thermal collector has been investigated as part of research that has been presented by Leonforte et al.. This infrastructure has been utilized to provide a residential building with cooling, heating, and hot water. According to the findings of this research, the collector both thermal and electrical efficiencies, as well as the performance of the heat pump throughout the seasons have both improved. Also, the amount of electricity exchanged with the grid is reduced in these conditions. The authors claim that this system is suitable for carbon zeroing residential buildings [16]. Chen et al. demonstrated the environmental, energy, and economic multi-objective optimization of a CPVT cogeneration setup that provides energy for an office building. The highlight of this study's results shows 41.4% and 41.7% better energy performance and adverse ecological effects. The proposed system provides 62% heating, 54% cooling, and only 30% electrical energy demands of the building [17].

Solar energy has been subjected to countless numbers of studies. The majority of these studies focus on the collecting methods of solar energy, such as thermal, PV, concentrating thermal, CPV, and CPVT collectors configuration. Adaptation of the solar system, which provides thermal energy, generated a new field of study in which this thermal energy is incorporated into intertwined systems to provide desirable outputs Based on the number output. These systems are classified into three major segments: cogeneration, trigeneration, and poly generation. In recent years, poly generation has attracted considerable attention due to its ability to improve the overall efficiency of systems. As a result, these systems are started gaining ground in the solar systems. The most efficient solar collector is the CPVT

collector, based on researches results. Limited numbers of studies are conducted on a combination of solar CPVT collectors with poly generation systems; the most crucial factor in this phenomenon is the fact that the CPVT becomes less efficient as the temperature of the medium rises. This issue was rectified by the triple-junction solar cell, which had better electrical efficiency and reduced the CPVT systems' dependence on temperature for this particular parameter. This system can provide a residential building energy demands; in this case, the poly generation system must consist of hot water, air heating, and air cooling, surplus to electrical generation. Different cooling structures can be adopted; among them, a single effect water ammonium absorption chiller due to its required working temperature seems promising. To the best of the authors, there is no previse attempt at economic and energy investigation of a CPVT-powered poly generation system underload of a residential building simultaneously.

The present study analyzes a poly generation solar system for a residential building located west of Tehran, Iran. In this study, a linear Fresnel reflector (LFC) is modeled as the concentration unit of a concentration photovoltaic thermal (CPVT) structure. Additionally, a NH3-H2O single effect absorption refrigeration chiller is modeled in essence to assess the amount of cooling energy that is generated by the system. Utilizing the engineering equation solver (EES) to generate the provided models' code, TRNSYS is coupled to EES so that transient simulation may occur. The residential building is simulated dynamically in the TRN-build subprogram of TRNSYS. The first thing that has to be done with this inquiry is to determine whether or not the solar system has the capability to fulfill the building's energy requirements so that it can be considered sustainable. The second objective is to analyze the system from an economic standpoint. Over the course of 22 years, an inspection of the structure's financial viability has been undertaken. Several distinct kinds of solar collectors are included into the framework that is being offered, and comparative studies of the design that is being presented are carried out.

2. METHODOLOGY

An overview of the proposed concept

The objective of the suggested structure is to provide air conditioning and hot water power requirements using solar energy for a residential building as well as power for the grid. The suggested system comprises of focusing solar reflectors that concentrate sunbeams to the absorber plate of collectors. The absorber plates comprised photovoltaic panels mounted on a thermal absorber plate. Ten tubes are integrated underneath a plate used to transport thermal energy to a solar working fluid in a thermal absorber plate configuration. The electrical output of the mechanism is offered to the grid, while the thermal power production of the solar arrangement is converted to heating or cooling cycles dependent on the building's energy requirement. The proposed heating cycle is adopted to provide air conditioning heating energy and the building hot water. Two auxiliary gas-fired heaters are incorporated in outlet hot water and outlet working fluid to the air-conditioning to provide the required energy when the solar system energy is insufficient. A water ammonium single effect absorption is assumed to satisfy the building's cooling energy needs. The solar cycle's thermal power is routed to the absorption chiller generator to fulfill the building's cooling

complex's needs. In the event that the energy provided by the sun is insufficient, a gas-powered auxiliary heater will be put into operation. Fig. 1 depicts this system's structural schematic.

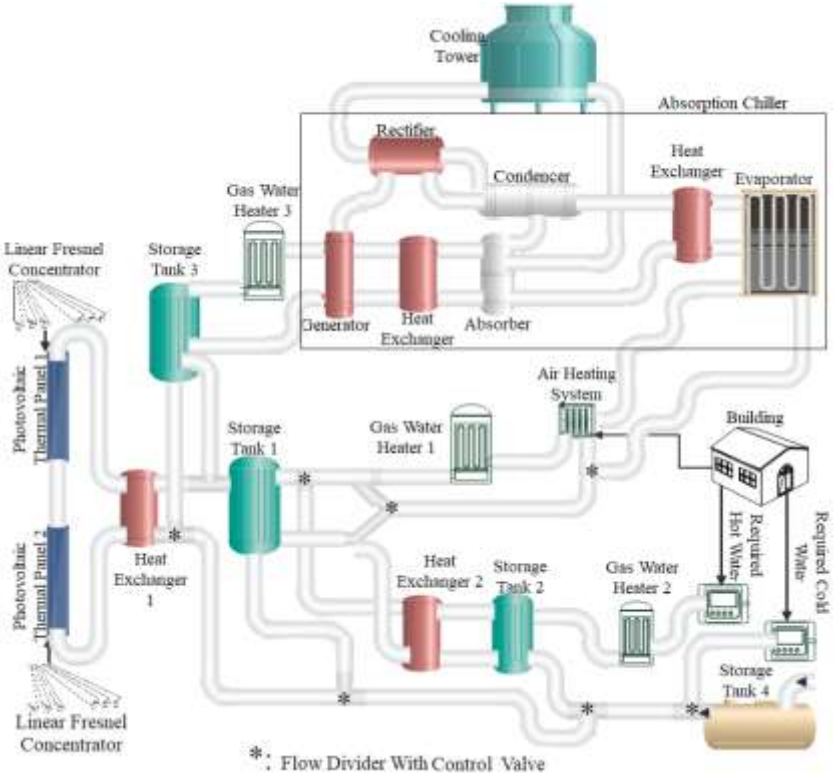

Fig. 1. Proposed system configuration schematic

The Linear Fresnel concentrator (LFC) is considered the system's concentrating unit. Specification of adopted LFC is presented in Table 1. There is two LFC utilized for this system. Due to mirror length, two series of the LFC's absorbers are considered for each LFC unit. The absorbers of the LFC are made up of a thermal absorber plate in addition to a photovoltaic panel that contains multiple junction solar cells. Table 2 Presents the multi-junction solar cell parameters. Aluminum Nitride with heat transfer conductivity of 1116 [kJ/hr m K] is considered for thermal absorber plate. Characteristics of the working fluid of the solar cycle are shown in Table 3. The heat exchangers adopted in this system have 700 [W/K] total heat transfer conditions.

Table 1. LFC module properties [18]

Parameter	Length (m)	Width (m)	Height receiver (m)	Standard optical efficiency	Mirror width (m)	Mirror length (m)	Concentration (sun)
Value	3.6	5.0	2.72	0.95	0.25	1.4	16

Table 2. solar photovoltaic module properties [19]

Parameter	Type	Efficiency (%)	Temperature	Radiation	Absorption	Conductivity

			efficiency modifier (1/°C)	efficiency modifier (1/kW)	coefficient (%)	coefficient (W/mK)
Value	triple-junction	15.8	0.002	0.0074	92	167

Table 3. The solar working fluid properties.

Parameter	Type	Operating temperature range (K)	Thermal conductivity (kj/m.K)	Density (kg/m3)	Heat capacity (W/kg-K)
Value	DURATHERM 450	248 to 505	0.5076	844	0.6111

Four storage tanks are employed in the proposed structure. Storage tanks number 1, 2, and 3 in the system's schematic Fig. 1 are constant volume thermal energy storage with a 5 cm polyurethane foam insulator. This insulator layer generates thermal resistance of 1.92 m2K/W for the storage tanks [20]. Storage tank number 4 is underground variable volume storage used to supply the building water.

Three auxiliary heaters are used to provide energy when solar energy is insufficient. These auxiliaries are gas-fired heaters with water as working fluid.

A water ammonium single-effect absorption chiller that has a coefficient of performance (COP) of 0.62 and a cooling capacity of 5 kW is employed to provide cooling. Boudéhenn, et al. developed this chiller model [21]. The specifications of this chiller are presented in Table 4 and Table 5. Chiller's evaporator and absorber operate at 6.2 bar, and condenser and disrober work at 12.4 bar. The chiller's pump operates at 32°C with an energy consumption of 550 W to increase the solution pressure from 6.2 to 12.4 bar. The rich solution flow rate is 89 kg/h.

3 Ton cooling tower with characteristics described in Table 6 is utilized to provide cooling fluid for the absorption chiller.

Table 4. Inlet parameters of absorption chiller [22]

	Heating fluid		Cooling fluid		Refrigerating fluid	
Parameter	Temperature (°C)	Flow rate (kg/h)	Temperature (°C)	Flow rate (kg/h)	Temperature (°C)	Flow rate (kg/h)
Value	95	144	30	158	14	136

Table 5. Chiller component properties [21]

	Evaporator		Condenser		Absorber		Disrober	
Parameter	Power (kW)	Temperature (°C)	Power (kW)	Temperature (°C)	Power (kW)	Temperature (°C)	Power (kW)	Temperature (°C)
Value	5	4	5	30	7.5	30	8	90

Table 6. cooling tower properties

Parameter	Cooling capacity (kW)	Air volume (CFM)	Operating weight (kg)	Dry weight (kg)	Power (HP)
Value	13	870	73	28	0.17

The building investigated in this study is a 110 m2 single-story residential building with a height of 3 m. A family of four live in this flat roof building. Two family members work outside 6 to 14 five days a week. Characteristics of the construction material of the building are presented in Table 7. It is estimated that this building has a ventilation rate of 0.4 each hour., and comfortable temperatures for winter and summer are 24 and 26°C, respectively.

Table 7. Parameters of the building components [23]

	External wall	Roof	Floor
Materials	1. Plaster 1.27 cm 2. Brick 10.16 cm 3. Plaster 1.27 cm	1. Asphalt 0.25 cm 2. Concrete 7.62 cm 3. Cement block 20.32cm 4. Plaster 1.27 cm	1. Plaster 1.27 cm 2. Cement block 20.32cm 3. Concrete 10.16 cm 4. Tile 2.54 cm
U-value (W/m2K)	3.8	1.9	0.34
Weight (kg/m2)	385	337	340

Energy evaluation of concentrating unit and absorption chiller
Using the following equation, one is able to determine the amount of incident energy from the sun that the linear Fresnel reflector is generated on a receiver.

$$G_{PVT} = \eta_{Opt}. I_b. IAM_{LFC}. C_{LFC} \quad (1)$$

Where GPVT, ηOpt, Ib, IAMLFC, and CLFC, are incident solar radiative, optical efficiency, beam radiation, LFC incidence angle modifier, and concentration ratio of LFC, respectively. Bellos and Tzivanidis developed the following equations to calculate the LFC incidence angle modifier [24].

$$\mathrm{IAM_{LFC}} = \mathrm{K_T}(\theta_\mathrm{T}).\mathrm{K_L}(\theta_\mathrm{L}) \tag{2}$$

Where θT, θL, KT, and KL are transversal solar incident angle, longitude solar incident angle, transversal incident angle modifier, and longitudinal incident angle modifier, respectively. The proposed longitudinal incident angle modifier of LFC is:

$$\mathrm{K_L}(\theta_\mathrm{L}) = -\frac{\mathrm{F}}{\mathrm{L}}\sqrt{1+\left(\frac{\mathrm{w}}{4\mathrm{F}}\right)^2.\sin(\theta_\mathrm{L})} \ +\cos(\theta_\mathrm{L}) \tag{3}$$

Where F, L, and W are focal length, LFC length, and the center and the last mirror of LFC distance, respectively.
The proposed Transversal solar incident angle modifier of LFC is:

$$\mathrm{K_T}(\theta_\mathrm{T}) = \begin{cases} \cos\left(\frac{\theta_\mathrm{T}}{2}\right) - \frac{\frac{\mathrm{w}}{4}}{\mathrm{F}+\sqrt{\mathrm{F}^2+\left(\frac{\mathrm{W}}{4}\right)^2}}\sin\left(\frac{\theta_\mathrm{T}}{2}\right) \\ \left[\cos\left(\frac{\theta_\mathrm{T}}{2}\right) - \frac{\frac{\mathrm{w}}{4}}{\mathrm{F}+\sqrt{\mathrm{F}^2+\left(\frac{\mathrm{W}}{4}\right)^2}}\sin\left(\frac{\theta_\mathrm{T}}{2}\right)\right].\frac{\mathrm{D_w}}{\mathrm{W_0}} \ .\frac{\cos(\theta_\mathrm{T})}{\cos\left(\frac{\theta_\mathrm{T}+\varphi_\mathrm{m}}{2}\right)} \end{cases} \tag{4}$$

Where Dw, and W0 are LFC reflectors distance, and LFC each mirror width.
φm position angle of the LFC mirrors is:

$$\varphi_\mathrm{m} = 2\arctan\left(\frac{\frac{\mathrm{W}}{4}}{\mathrm{F}+\sqrt{\mathrm{F}^2+\left(\frac{\mathrm{W}}{4}\right)^2}}\right) \tag{5}$$

θT,crit critical transversal solar angle, after which shading effects starts is:

$$\theta_\mathrm{T,crit} = 94.46 - 2.519.\lambda - 55.71.\lambda^2 - 0.48.\varphi_\mathrm{i} + \frac{1.77\varphi_\mathrm{i}}{1000} + 1.15.\lambda.\varphi_\mathrm{i} \tag{6}$$

Where λ is the width to the distance ratio of the LFC mirror.

It is possible to express transversal and longitudinal incidence angles as a function of solar zenith and azimuth angles using the following formula:

$$\theta_T = \arctan(|\sin(\gamma_s)|.\tan(\theta_z)) \quad (7)$$

$$\theta_L = \arctan(\cos(\gamma_s).\tan(\theta_z)) \quad (8)$$

Where γs, and θz are the solar azimuth and zenith angles, respectively.
The absorption chiller is made up of a generator, absorber, condenser, evaporator, expansion valves, pump, rectifier, and heat exchangers. Fig. 2. illustrates the suggested single-effect absorption chiller concept.

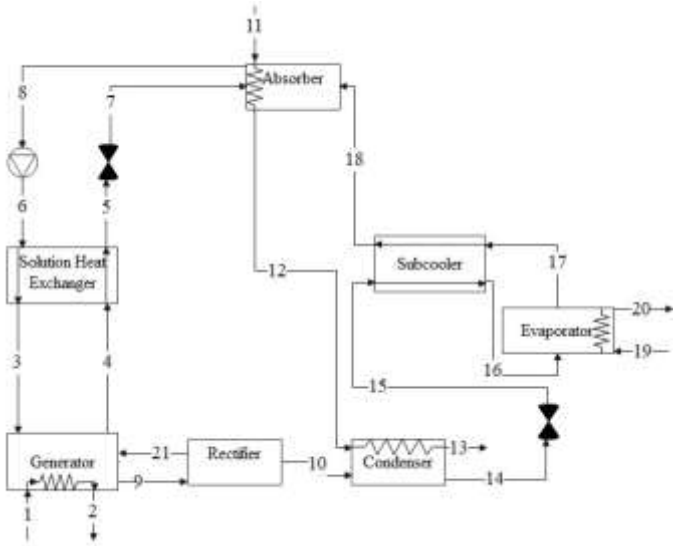

Fig. 2. single-effect absorption chiller schematic

The models developed by Sirwan et al. and Kızılkan et al. to evaluate absorption chillers are implemented in order to generate utilized single-effect water ammonium absorption chiller. The proposed absorption chiller's energy and mass balance with consideration of a binary mixture of NH3-H2O are presented in fallow.
Energy and mass balance for generator:

$$\dot{m}_{21} + \dot{m}_3 = \dot{m}_4 + \dot{m}_9 \quad (9)$$

$$\dot{m}_{21}.X_{21} + \dot{m}_3.X_3 = \dot{m}_4.X_4 + \dot{m}_9.Y_9 \quad (10)$$

$$\dot{Q}_G = \dot{m}_1.h_1 + \dot{m}_2.h_2 = \dot{m}_4.h_4 + \dot{m}_9.h_9 - \dot{m}_{21}.h_{21} - \dot{m}_3.h_3 \quad (11)$$

Where h, X, Y, m, and Q˙G are specific enthalpy, liquid solution concentration, vapor solution concentration, mass flow rate, and generator heat transfer rate, respectively.
Energy and mass balance for solution heat exchanger:

$$\dot{m}_4 = \dot{m}_5 \qquad X_4 = X_5 \qquad \dot{m}_6 = \dot{m}_3 \qquad X_3 = X_6 \quad (12)$$

$$\dot{Q}_{HEX} = \dot{m}_3.h_3 - \dot{m}_6.h_6 = \dot{m}_4.h_4 - \dot{m}_5.h_5 \quad (13)$$

The rate of heat transfer happening inside the heat exchanger is denoted by Q˙HEX.
Balance of energy and mass for solution pump:

$$\dot{m}_8 = \dot{m}_6 \qquad X_8 = X_6 \tag{14}$$

$$\dot{w}_p = \dot{m}_6.h_6 - \dot{m}_8.h_8 = \dot{m}_8.v_8.(P_H - P_L) \tag{15}$$

Where w˙p, PH, PL, and v are pump work, generator pressure, absorber pressure, and solution specific volume, respectively.
Energy and mass balance for expansion valves:

$$\dot{m}_5 = \dot{m}_7 \qquad X_5 = X_7 \qquad h_5 = h_7 \tag{16}$$

$$\dot{m}_{14} = \dot{m}_{15} \qquad X_{14} = X_{15} \qquad h_{14} = h_{15} \tag{17}$$

Energy and mass balance for absorption:

$$\dot{m}_8 = \dot{m}_7 + \dot{m}_{18} \tag{18}$$

$$\dot{m}_8.X_8 = \dot{m}_7.X_7 + \dot{m}_{18}.X_{18} \tag{19}$$

$$\dot{Q}_{Ab} = \dot{m}_7.h_7 + \dot{m}_{18}.h_{18} - \dot{m}_8.h_8 = \dot{m}_{12}.h_{12} - \dot{m}_{11}.h_{11} \tag{20}$$

Where Q˙Ab is absorber heat transfer rate.
Energy and mass balance for sub-cooler:

$$\dot{m}_{17} = \dot{m}_{18} \qquad X_{17} = X_{18} \qquad \dot{m}_{15} = \dot{m}_{16} \qquad X_{15} = X_{16} \tag{21}$$

$$\dot{Q}_{subC} = \dot{m}_{15}.h_{15} - \dot{m}_{16}.h_{16} = \dot{m}_{18}.h_{18} - \dot{m}_{17}.h_{17} \tag{22}$$

The heat transfer rate via the sub-cooler is denoted with Q˙subC.
The evaporator's energy and mass balances are as follows:

$$\dot{m}_{17} = \dot{m}_{16} \qquad X_{17} = X_{16} \qquad \dot{m}_{20} = \dot{m}_{19} \tag{23}$$

$$\dot{Q}_{EV} = \dot{m}_{17}.h_{17} - \dot{m}_{16}.h_{16} = \dot{m}_{20}(h_{19} - h_{20}) \tag{24}$$

The rate of heat transfer in the evaporator is denoted by Q˙EV.
The condenser's energy and mass balances are as follows:

$$\dot{m}_{10} = \dot{m}_{14} \qquad X_{10} = X_{14} \tag{25}$$

$$\dot{Q}_{Co} = \dot{m}_{10}.h_{10} - \dot{m}_{14}.h_{14} = \dot{m}_{10}(h_{13} - h_{12}) \tag{26}$$

The rate of heat transfer in the evaporator is indicated by Q˙Co.
Adopting concepts of LMTD (logarithmic mean temperature difference) and UA (overall heat transfer coefficient), each component of the absorption chiller heat transfer rate can be expressed as follow:

$$EF_G = \frac{T_1 - T_2}{T_1 - T_9} \quad (27)$$

$$LMTD_G = \frac{(T_1 - T_4) - (T_2 - T_9)}{Ln(\frac{(T_1 - T_4)}{T_2 - T_9})} \quad (28)$$

$$\dot{Q}_G = LMTD_G . UA_G \quad (29)$$

$$LMTD_{HEX} = \frac{(T_4 - T_3) - (T_6 - T_5)}{Ln(\frac{(T_4 - T_3)}{T_6 - T_5})} \quad (30)$$

$$\dot{Q}_{HEX} = LMTD_{HEX} . UA_{HEX} \quad (31)$$

$$EF_{Ab} = \frac{T_{12} - T_{11}}{T_8 - T_{11}} \quad (32)$$

$$LMTD_{Ab} = \frac{(T_8 - T_{12}) - (T_7 - T_{11})}{Ln(\frac{(T_8 - T_{12})}{T_7 - T_{11}})} \quad (33)$$

$$\dot{Q}_{Ab} = LMTD_{Ab} . UA_{Ab} \quad (34)$$

$$LMTD_{SubC} = \frac{(T_{17} - T_{16}) - (T_{15} - T_{18})}{Ln(\frac{(T_{17} - T_{16})}{T_{15} - T_{18}})} \quad (35)$$

$$\dot{Q}_{SubC} = LMTD_{SubC} . UA_{SubC} \quad (36)$$

$$EF_{EV} = \frac{T_{19} - T_{20}}{T_{19} - T_{17}} \quad (37)$$

$$LMTD_{EV} = \frac{(T_{19} - T_{17}) - (T_{20} - T_{17})}{Ln(\frac{(T_{19} - T_{17})}{T_{20} - T_{17}})} \quad (38)$$

$$\dot{Q}_{EV} = LMTD_{EV} . UA_{EV} \quad (39)$$

$$EF_{Co} = \frac{T_{12} - T_{13}}{T_{12} - T_{14}} \quad (40)$$

$$LMTD_{Co} = \frac{(T_{14} - T_{12}) - (T_{14} - T_{13})}{Ln(\frac{(T_{14} - T_{12})}{T_{14} - T_{13}})} \quad (41)$$

$$\dot{Q}_{Co} = LMTD_{Co} . UA_{Co} \quad (42)$$

COP, coefficient of performance of this absorption chiller is:

$$COP = \frac{\dot{m}_{19}(h_{19} - h_{20})}{\dot{m}_1(h_1 - h_2)} \quad (43)$$

Economical assessment

A detailed components costs of the concentrated solar room heating and cooling with supplying hot water and power are presented in Table 8.

Table 8. Proposed system equipment costs

component	Specific cost ($)	Utilized units	cost ($)	Total Share (%)	Reference
PVT	350/m2	1.8 m2	630	2.99%	[25]
LFC field	200/m2	36 m2	7200	40%	[26]
TES	1250/ m3	1.5 m3	1875	9.99%	[26]
Thermal oil	2/ kg	30 kg	60	0.01	[26]
Piping	30/ m2 (collector area)	1.8 m2	54	0.01	[26]
Heat exchanger	100	2	200	1	[27]
Auxiliary heater	107	2	214	1	[27]
Auxiliary heater water	5	1	5	0.01	[27]
Pump	$1026\ \left(\frac{\dot{w}_p}{300}\right)^{0.25}$	20 kW	521	3%	[28]
Absorption Chiller	$14740.2\ \dot{Q}_{EV}^{\ -0.6849} + 3.3$	5 kW	4899	27%	[28]
Cooling tower	2000	1	2000	11%	-
Controlling system	500	1	500	2.99%	-
Total	-	-	18158	100	-

When calculating the entire amount of profit that may be made from a system, net present value, also known as NPV, is utilized since it takes into account the temporal worth of the investment. Two of the essential factors which affect the NPV are the discount rate and projected returns. These parameters' predictive nature is the primary cause of uncertainty in the results. NPV can be presented as:

$$\mathrm{NPV} = -\mathrm{C}_0 + \sum_{0}^{\mathrm{p=m-1}} \frac{\mathrm{R}_p}{(1+\mathrm{i})^p} \tag{44}$$

Where C0, Rt, t, and i are the initial costs, period t net cash flow, number of periods, and interest rate, respectively. The rate of interest at which an investment's net present value is equivalent to zero is known as the internal rate of return (IRR). Net present costs (NPC) and net present benefit (NPB) are two crucial parameters for the financial evaluation of the scheme.

The benefit-to-cost ratio, often known as the BCR, is an excellent indicator of the system's current financial state. It may be expressed as follows:

$$\mathrm{BCR} = \frac{\mathrm{NPB}}{\mathrm{NPB}} \tag{45}$$

The Levelized Cost of Energy (LCOE) parameter evaluates alternative energy production methods. The LCOE determines if the system will break even or not. This parameter represents the total operating costs for the entire energy production of the system as follow:

$$\mathrm{LOEC} = \frac{\sum_{0}^{\mathrm{p=m-1}} \frac{\mathrm{c_t}}{(1+\mathrm{i})^p}}{\sum_{0}^{\mathrm{p=m-1}} \frac{\mathrm{E_t}}{(1+\mathrm{i})^p}} \tag{46}$$

Where ct, and Et are system cost and energy production in the period.

3. SIMULATION

The TRNSYS is a well-known renewable energy softer assessment for the transient condition utilized for academic and commercial applications [29]. This software can use other applications such as engineering equation solver (EES). EES is one of the best thermodynamic and mathematical evaluations program [30]. Adaptation of the SketchUp design building in the TRNSYS provides the meaning for energy evaluation of the building.

The system's modeling inquorate Type15-2 provides the weather data as the system's initial conditions. The specification data input of Type15-2 is the whether conditions of Tehran. For modeling LFC with the solar beam radiation, incident angle, solar zenith, and azimuth angles transfer to EES by Type66a and an EES code based on Eq. 1 to 8 return concentrated solar radiation on the unit of area. Required parameters of the utilized equation are presented in the LFC specifications. Type 563 is chosen to model the PVT unit of the system. Characteristics for this component are the combination of the PV module, synthetic oil, and thermal absorber. Type 563 generates the CPVT system's electrical power and temperature outputs when input temperature and radiation are provided. Type3b is adapted to model the system pumps. On account of the ephemeral nature of solar cycles, the system has three TES. These storage tanks have 0.5 m3 and are modeled by Type158. Auxiliary heaters are another safety mechanism to counteract the temporary nature of solar energy and generate the required energy for the building. Type700 provides the model for this element. The closed loped system has a better life span than open lope ones. Based on this fact, heat exchangers are adapted to separate different systems parts. The counter flow heat exchangers of the proposed system are modeled inquiring Type5b. A 1 m3 underground storage tank model by Type39 is selected to provide domestic water.

An EES code based on Eq. 9 to 43 is generated to simulate the absorption chiller. The inlet parameter for this model transfers to EES with Type66a, and outlet conditions are returned. Type128 is proposed for the cooling tower. The building energy model is assisted using Type56 –TRNBuild. Type682 is used to link the building energy result to the system. Fig. 1 demonstrates the proposed system schematic in the TRNSYS. The economic assessment of the system is carried out by first extracting the electrical productivity of the PVT units, then

adopting the costs of the system, and finally taking into account the thermal energy that is produced by the solar cycle for both heating and cooling. This parameter transfers to an EES code base of Eq. 44 to 46.

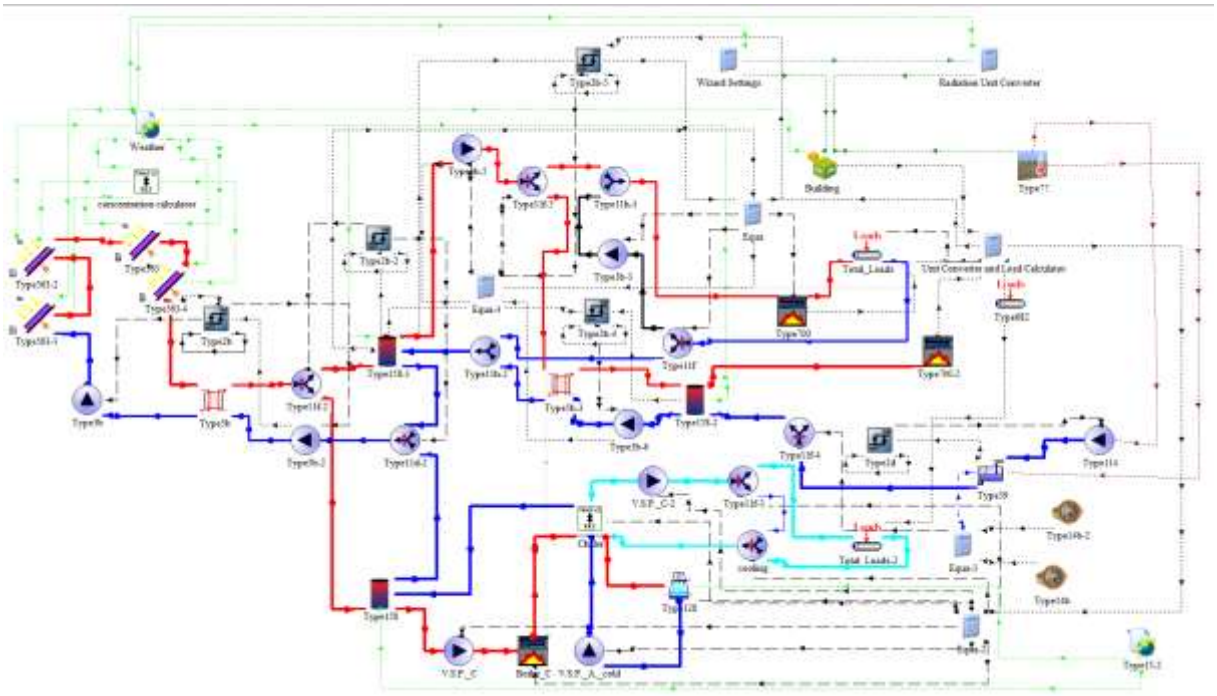

Fig. 3. The proposed system schematic in the TRNSYS

4. RESULTS AND DISCUSSIONS

validation

Models utilized to describe system conditions require validation to ensure the model's reliability. Considering the understudy system has three main segments for which valid study results are available, the model validation breaks down into the building, the LFC, and Concentrated solar tri-generation models. The Dependableness of the adopted model for building evaluation using Baneshi and Maruyama's study[25], the comparison of the present modeling data and those of the Baneshi and Maruyama are presented in Table 9. The analogy of this table data, based on the fact that most of the divergences arise from the difference in the adopted whether data, the conclusion of validity of the present model for the building's energy demand can be drawn.

Table 9. The present model of building energy demand compared to Baneshi and Maruyama's research [25]

	Peak cooling load (kW)	Peak heating load (kW)	Total cooling load (kWh)	Total heating load (kWh)
Reference value [25]	2.3	3.0	3080	6120
Study value	2.4	3.1	3387.4	6362.3
Divergence	4%	3%	9%	4%

The LFC's model heavily relies on longitudinal and transversal incidence angle modifiers to generate incidence angle modifier. Most LFC manufacturers provide longitudinal and transversal incidence angle modifiers for their products. Fig. 4 shows the presented model for LFC and manufacturer data presented in the research of Famiglietti and Lecuona [18]. This chart indicates that the current model and the reference data agree with one another astonishingly.

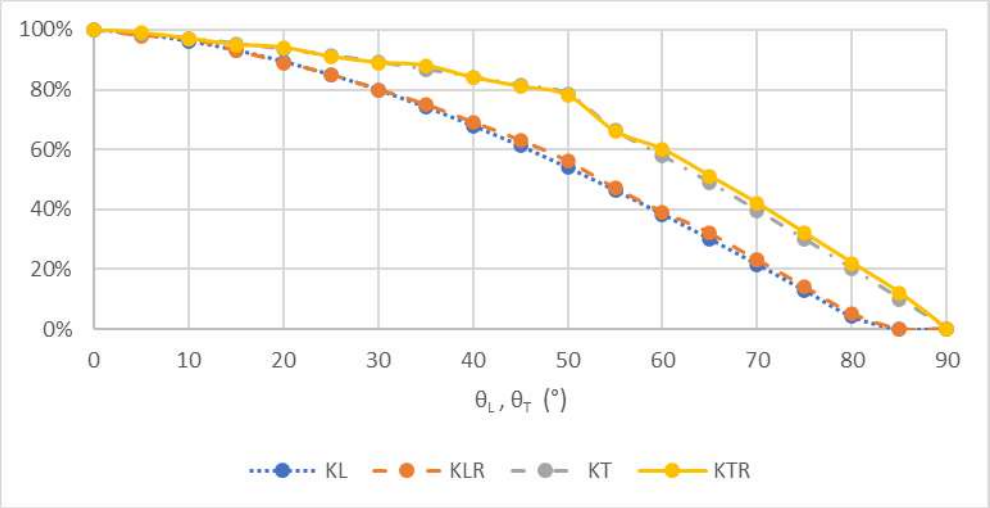

Fig. 4. The transversal and longitudinal incidence angle modifiers of this investigation were compared with the values that Famiglietti and Lecuona had obtained [18]

For the final stage of validation, with the separation of the CPVT from heating and cooling air conditioning simultaneously utilizing standard PV cells instead of triple-junction solar cells, the system transforms into the proposed design of Moaleman et al. [22]. Changing the other parameters of the system to those incorporated in Moaleman et al., a comparison of the present simulation and Moaleman et al. are illustrated in Table 10. The presented result of this table indicates the proposed model for the absorption chiller and LFC have a good agreement with the one adopted in the earlier mentioned research.

Table 10. comparison of overall energy generation of the proposed model for Moaleman et al. system with their data [22]

	Electrical energy production	Thermal energy production	Cooling energy production
Reference value [22]	2290 (kWh)	6528 (kWh)	3944 (kWh)
Study value	2423.5 (kWh)	6835.6(kWh)	4018.8 (kWh)
Divergence	6%	4%	2%

The proposed system's energy performance

In the first place, to eliminate the effects of initial conditions on the simulation, the simulation is conducted for 13 months, and the first month's data are neglected.

Fig. 5. A, B, C, and D, demonstrate the annual consumption of cooling and heating power

for the building, as well as the consumption of supplementary heating for either climate., respectively. The building's utmost heating and cooling demand occur at 7 AM on January 13th and 9 AM on August 19th, with 3.13 and 2.44 kW, respectively. The highest energy requirements of 3.68 kW for the heating system auxiliary and 3.94 kW for the cooling system auxiliary are needed at 7 AM on January 13th and 17:30 on July 22th, respectively. The efficiency of both the boiler and the combustion contributes to the greater energy expenditure of the auxiliary as compared to the energy usage of the building loads. Furthermore, the lower than one COP of the chiller increases contributes to this higher energy consumption in the cooling cycle.

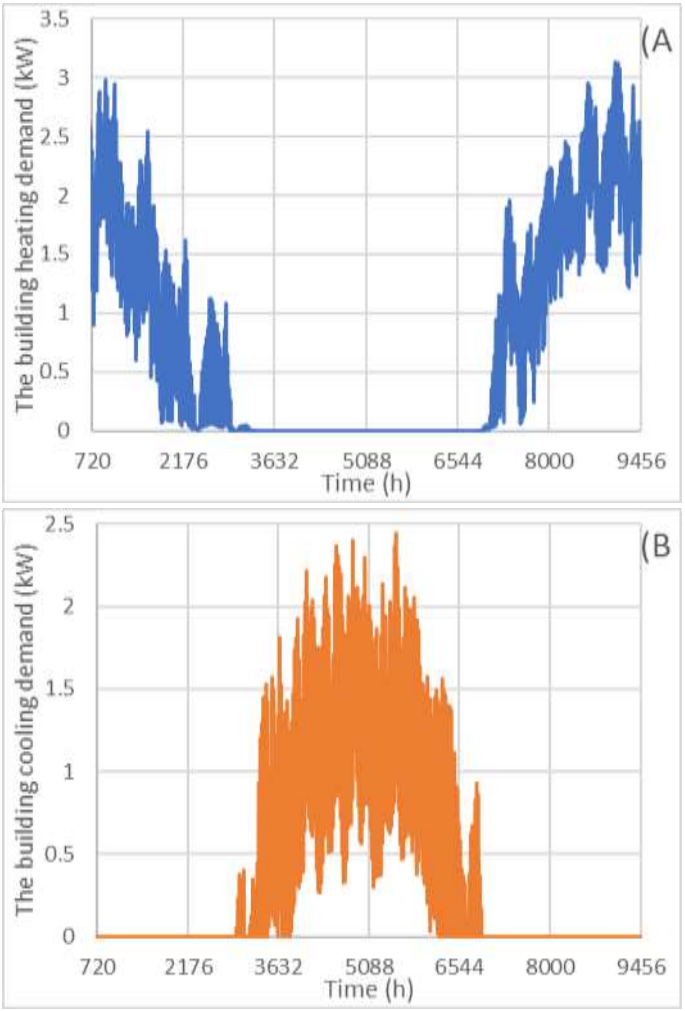

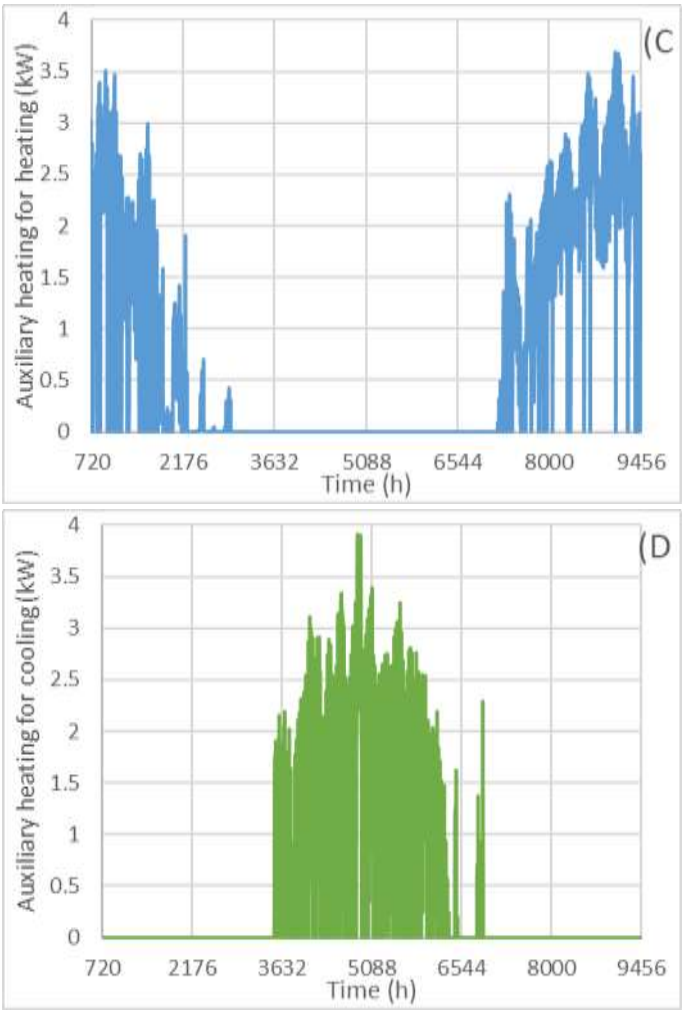

Fig. 5. The building's air-conditioning energy demands and required auxiliary heaters.

Fig. 6 A and B depict the CPVT's electrical and thermal power generation year-round. The energy creation of the CPVT unit is dependent upon the temperature of the PVT absorber plate and beam radiation. The temperature of the absorber plates of the CPVT is indirectly dependent on solar radiation. As expected, the system's maximum electrical and thermal energy productions are generated in summer with 5.48 and 11.34 kW, respectively. The proposed design can provide 98% of the energy required to generate municipal hot water for the building. The incoming municipal water is assumed to have the same temperature as the earth two miters underground. Fig. 7 A depicts the output temperature of the CPVT system over the course of a year. The control system of the proposed structure is coded to generate cooling if the outlet temperature of the CPVT reaches 160°C and dissipates excessive energy; consequently, the maximum outlet temperature of the CPVT cycle is restricted to 160°C. Although the present proposed design does not take advantage of CPVT passive cooling, the temperature results indicate the capability for such a system. Fig. 7 B, and C represent CPVT thermal and electrical efficiency. With increasing solar radiation, the thermal and electrical efficiency of the structure must grow. Still, an increase in temperature has an inverse effect on these parameters and cancels out the impact of solar radiation growth. Utilizing multijunction cells is directly responsible for the CPVT's high electrical efficiency (up to 28 percent), which converts solar energy to electrical energy more

efficiently. The control system maintains the building's temperature at 24°C in cold and 26°C in hot seasons. Air change infiltration of the building is assumed to be 0.4 in an hour.

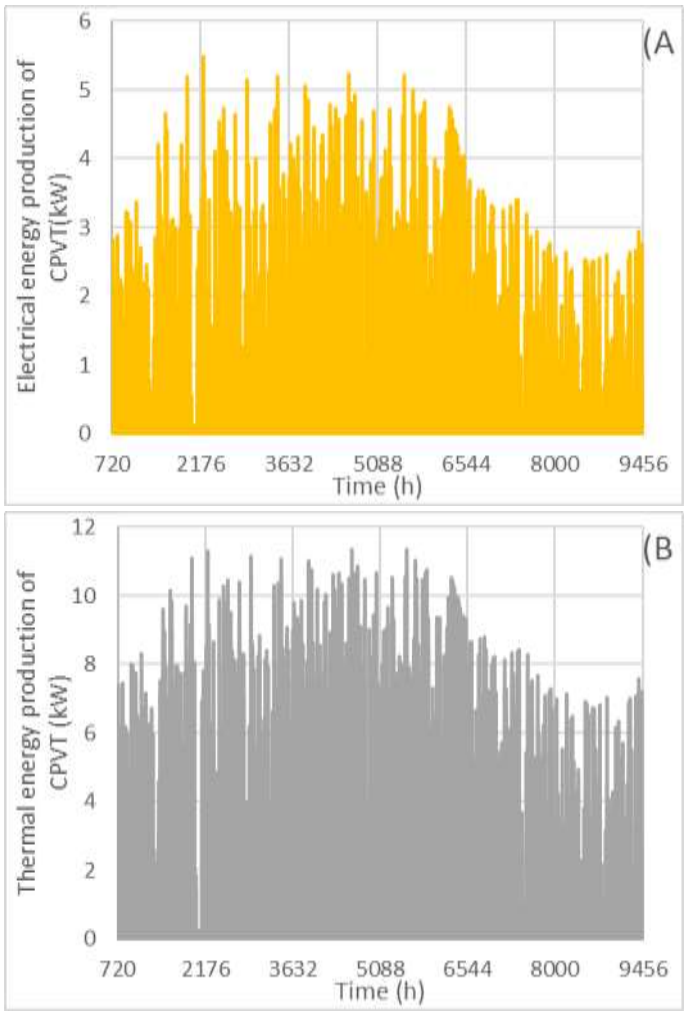

Fig. 6. Year-round electrical and thermal energy production via the CPVT system

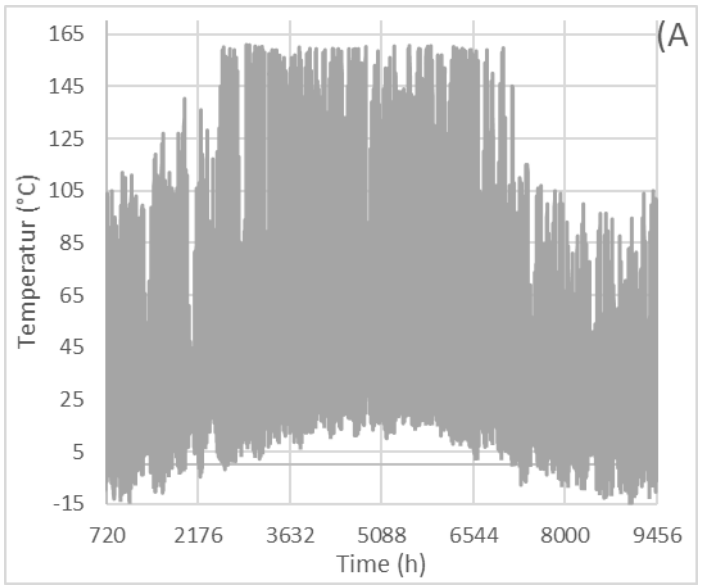

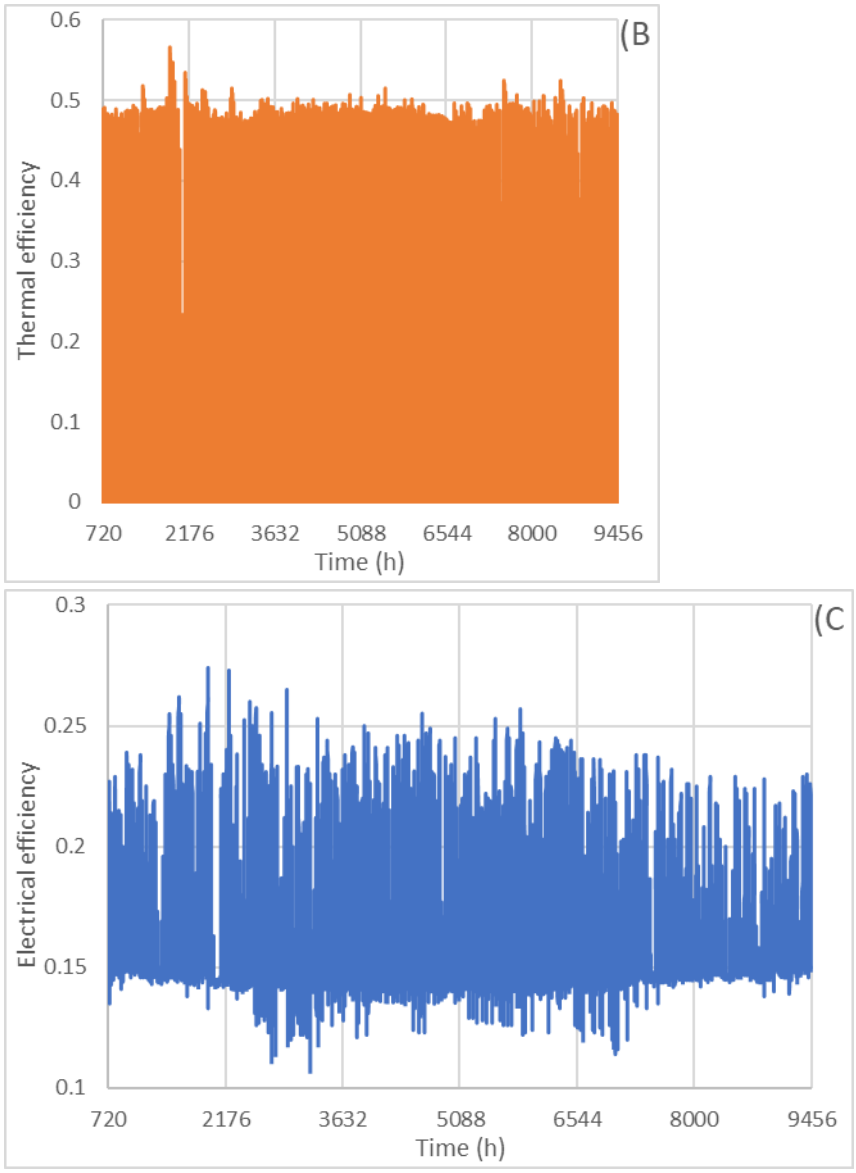

Fig. 7. Outlet temperature, thermal, and electrical efficiency of the CPVT during a year

A comparative assessment of different methods to provide the energy to satisfy the building energy demand is presented in Table 11. In this table, All systems, with the exception of two parallel CPVT with triple-junction solar cells, have the same collector area, whereas the final design has double the size of the others. PVT with standard solar cell structure is used as the reference for other structure energy evaluation. Utilizing this structure reduces the energy required for water heating by 71%. PVT with triple-junction solar cells requires 1% more energy for water heating and produces 12% more electrical energy than the standard solar system. However, a concentrated thermal collector has no electrical energy production but generates 418% more thermal energy. CPVT with normal solar cells provides 384% more thermal energy due to the adaptation of concentrating unit and 32% less electrical energy than the standard system. This reduction in electrical production is mainly due to the cell temperature increase in this system. CPVT with triple-junction solar cells avoids this negative effect by implementing cells with lower dependency on temperature. This structure has 25% and 366% higher electrical and thermal energy production. Combining two CPVT

with triple-junction solar cells in a parallel system, 114%, and 555% more electrical and thermal energy than the standard case can be obtained.

Table 11. Different types of the solar unit performance adopted in the proposed system

	Required auxiliary heater for the heating cycle (kWh)	Required auxiliary heater for water heating (kWh)	Required auxiliary heater for the cooling cycle (kWh)	Solar electrical energy production (kWh)	Solar thermal energy production (kWh)
No solar cycle	7484.96	3235.66	7277.32	0	0
PVT with standard solar cells	7484.96	950.10	7269.52	4476.71	3100.81
PVT with triple-junction solar cells	7484.96	955.58	7269.53	5036.08	3065.68
Concentrated thermal collector	5627.07	2866.26	8.86	0	16054.39
CPVT with standard solar cells	6006.78	3121.03	13.65	3052.21	15011.35
CPVT with triple-junction solar cells	6018.80	3377.65	13.37	5585.84	14437.60
Two parallel CPVT with triple-junction solar cells	4391.06	199.09	4.01	9578.08	20318.16

The proposed system's economic performance

The main assumptions are a 5% interest rate, a life span of 22 years for collectors, 0.216 $/kWh feed-in tariff, 0.033 $/m3 CNG price, and 0% tax [14]; economic factors for different solar collector configurations are presented in Table 12. With current government regulations regarding energy, CPVT with triple-junction solar cells has the best economical performance. All of the collectors, to some extent, have economic justification except for concentrated thermal collectors. The low-cost CNG is the most crucial factor that

significantly impacts this system's economic justification. Most of the solar cycle's revenue stems from electrical production.

Table 12. Economical parameters for different solar collectors utilized in the system.

	NPC ($)	Operating and maintenance costs ($)	NPV ($)	PBT (year)	BCR	IRR (%)	LCOE ($/kWh)
PVT with standard solar cells	10626	106.26	8953.54	11.03	84%	7%	0.025
PVT with triple-junction solar cells	16936	84.68	5509.13	15.33	33%	3%	0.028
Concentrated thermal collector	10410	208.2	-3873.40	-	-37%	-3%	0.018
CPVT with standard solar cells	10626	318.78	6363.57	12.71	60%	5%	0.022
CPVT with triple-junction solar cells	11040	276	17557.71	7.84	159%	12%	0.018
Two parallel CPVT with triple-junction solar cells	19040	476	26964.17	8.41	142%	11%	0.021

5. CONCLUSION

A solar poly generation system is subjected to investigation in the present study. The proposed system consists of concentrating photovoltaic thermal collectors, which in addition to electrical energy production to sell to the grid, partially provide thermal energy for air-conditioning unit and hot water. The proposed concentration system for collectors is a linear Fresnel reflector incorporating triple-junction solar cells. The system has gas-fired

backup heaters. The system directly utilizes the thermal energy to meet the building heating requirement, and in order to provide the building with the necessary cooling energy, a single effect ammonium water absorption chiller has been installed. Mathematical models for the LFC and absorption chiller are cared out and coded in EES. The system simulated incorporating a residential building located in the west of Tehran, Iran, in TRNSYS. Validation of the system's model is carried out compared to previse studies. Finally, system economics and energy performance are investigated. The most important results of this study can be highlighted as follow:

The suggested CPVT made with triple-junction solar cells has a thermal efficiency mean value of 48 percent and an electrical efficiency mean value of 23 percent.

The total energy production of the proposed concept of CPVT is 10%, 20%, 60%, and 62% higher than CPVT with standard solar cells, concentrated thermal collector, PVT with highly-efficient cells, and PVT with traditional solar cells, respectively.

The proposed CPVT for the system reduces building energy requirements by 48%. In contrast, CPVT with standard solar cells, concentrated thermal collectors, PVT highly-efficient cells, and PVT with traditional solar cells reduce these requirements by 49%, 53%, 13%, and 13%, respectively. These are regardless of the electrical production of each system.

Adopting two of the proposed CPVT connected parallelly to the system accounted for 74% of the system's energy demands.

The proposed CPVT has NPC, NPV, PBT, BCR, IRR, and LCOE of 11040, 17557, 7.84, 159%, 12%, and 0.018, respectively. This economic data indicates the system's low to medium economic attraction.

The most negative impact on the system's economic efficiency is the low-cost CNG, as a concentrated thermal collector has a -3% IRR and -3873.40 NPV, which are the indicators of investment Loss.

Nomenclature

BCR	Benefit-to-cost ratio	T	Temperature (°C)
C0	Initial costs ($)	t	Number of periods
CLFC	Concentration ratio of LFC	TES	Thermal energy storage
COP	Coefficient of performance of	UA	Overall heat transfer
Dw	absorption chiller	v	coefficient (kW/°C)
EF	LFC reflectors distance (m)	W	Specific volume of solution
F	efficiency	W0	(m3/kg)
GPVT	Focal length (m)	w ̇p	The center and the last
h	Incident radiative flow (W)	X	mirror of LFC distance (m)
i	Specific enthalpy (kJ/kg)	Y	LFC each mirror width (m)
IAMLFC	Interest rate		Pump work (kW)
Ib	Incidence angle modifier of	γs	Liquid solution
IRR	LFC	ηOpt	concentration
LCOE	Beam radiation (W/m2)	θL	Vapor solution
LMTD	Internal rate of return (%)	θT	concentration
IRR	Levelized Cost of Energy	θz	Greek symbols

KL	Logarithmic mean temperature difference (°C)	λ	Solar azimuth angle (°)
KT	Internal rate of return	φm	Optical efficiency
L	Longitudinal incident angle modifier of LFC	Ab	Longitudinal incident angle (°)
LCOE	Transversal solar incident angle modifier of LFC	Co	Transversal incident angle (°)
m˙	LFC length (m)	EV	Solar zenith angle (°)
NPB	Levelized cost of energy ($/kWh)	G	The width to the distance ratio of the LFC mirror
NPC	Mass flow rate (kg/h)	H	Position angle of the LFC mirrors (°)
NPV	Net present benefit ($)	HEX	subtitles
P	Net present costs ($)	L	Absorber
PBT	Net present value ($)	subC	Condenser
Q	Pressure (kPa)		Evaporator
Rt	Payback time (year)		Generator
	Heat transfer rate (kW)		high
	Period t net cash flow ($)		Heat exchanger
			Low
			Sub cooler

REFERENCES

1. Wrigley EA. Energy and the English Industrial Revolution. Philosophical Transactions of the Royal Society A: Mathematical, Physical and Engineering Sciences. 2013;371(1986):20110568.
2. Adams WG, Day RE. V. The action of light on selenium. Proceedings of the Royal Society of London. 1877;25(171-178):113-7.
3. Hansen J, Sato M, Ruedy R, Lacis A, Oinas V. Global warming in the twenty-first century: An alternative scenario. Proceedings of the National Academy of Sciences. 2000;97(18):9875-80.
4. Thirugnanasambandam M, Iniyan S, Goic R. A review of solar thermal technologies. Renewable and sustainable energy reviews. 2010;14(1):312-22.
5. Quaschning V, Muriel MB. Solar power-photovoltaics or solar thermal power plants? VGB POWERTECH-INTERNATIONAL EDITION-. 2002;82:48-52.
6. Tselepis S, Tripanagnostopoulos Y, editors. Economic analysis of hybrid photovoltaic/thermal solar systems and comparison with standard PV modules. Proceedings of the international conference PV in Europe; 2002.
7. Huang BJ, Lin TH, Hung WC, Sun FS. Performance evaluation of solar photovoltaic/thermal systems. Solar Energy. 2001;70(5):443-8.
8. Coventry JS. Performance of a concentrating photovoltaic/thermal solar collector. Solar Energy. 2005;78(2):211-22.
9. Theristis M, Fernández EF, Stark C, O'Donovan TS. A theoretical analysis of the impact of atmospheric parameters on the spectral, electrical and thermal performance of a concentrating III–V triple-junction solar cell. Energy Conversion and Management.

2016;117:218-27.
10. Mittelman G, Kribus A, Dayan A. Solar cooling with concentrating photovoltaic/thermal (CPVT) systems. Energy Conversion and Management. 2007;48(9):2481-90.
11. Mittelman G, Kribus A, Mouchtar O, Dayan A. Water desalination with concentrating photovoltaic/thermal (CPVT) systems. Solar Energy. 2009;83(8):1322-34.
12. Buonomano A, Calise F, Palombo A. Solar heating and cooling systems by CPVT and ET solar collectors: A novel transient simulation model. Applied Energy. 2013;103:588-606.
13. Horvat I, Grubišić D, Marušić A, Lončar D. Operation Strategies of a Solar Trigeneration Plant in a Residential Building. Journal of Sustainable Development of Energy, Water and Environment Systems. 2021;9(2):1-13.
14. Deymi-Dashtebayaz M, Rezapour M, Farahnak M. Modeling of a novel nanofluid-based concentrated photovoltaic thermal system coupled with a heat pump cycle (CPVT-HP). Applied Thermal Engineering. 2022;201:117765.
15. Calise F, Cappiello FL, Dentice d'Accadia M, Vicidomini M. Thermo-economic optimization of a novel hybrid renewable trigeneration plant. Renewable Energy. 2021;175:532-49.
16. Leonforte F, Miglioli A, Del Pero C, Aste N, Cristiani N, Croci L, et al. Design and performance monitoring of a novel photovoltaic-thermal solar-assisted heat pump system for residential applications. Applied Thermal Engineering. 2022;210:118304.
17. Chen Y, Hu X, Xu W, Xu Q, Wang J, Lund PD. Multi-objective optimization of a solar-driven trigeneration system considering power-to-heat storage and carbon tax. Energy. 2022;250:123756.
18. Famiglietti A, Lecuona A. Small-scale linear Fresnel collector using air as heat transfer fluid: Experimental characterization. Renewable Energy. 2021;176:459-74.
19. Helmers H, Kramer K. Multi-linear performance model for hybrid (C)PVT solar collectors. Solar Energy. 2013;92:313-22.
20. Fantucci S, Lorenzati A, Kazas G, Levchenko D, Serale G. Thermal Energy Storage with Super Insulating Materials: A Parametrical Analysis. Energy Procedia. 2015;78:441-6.
21. Boudéhenn F, Demasles H, Wyttenbach J, Jobard X, Chèze D, Papillon P. Development of a 5 kW cooling capacity ammonia-water absorption chiller for solar cooling applications. Energy Procedia. 2012;30:35-43.
22. Moaleman A, Kasaeian A, Aramesh M, Mahian O, Sahota L, Nath Tiwari G. Simulation of the performance of a solar concentrating photovoltaic-thermal collector, applied in a combined cooling heating and power generation system. Energy Conversion and Management. 2018;160:191-208.
23. Baneshi M, Maruyama S. The impacts of applying typical and aesthetically–thermally optimized TiO2 pigmented coatings on cooling and heating load demands of a typical residential building in various climates of Iran. Energy and Buildings. 2016;113:99-111.
24. Bellos E, Tzivanidis C. Development of analytical expressions for the incident angle modifiers of a linear Fresnel reflector. Solar Energy. 2018;173:769-79.
25. Matuska T. Performance and economic analysis of hybrid PVT collectors in solar DHW system. Energy Procedia. 2014;48:150-6.

26. Cocco D, Cau G. Energy and economic analysis of concentrating solar power plants based on parabolic trough and linear Fresnel collectors. Proceedings of the Institution of Mechanical Engineers, Part A: Journal of Power and Energy. 2015;229(6):677-88.
27. Ala G, Orioli A, Di Gangi A. Energy and economic analysis of air-to-air heat pumps as an alternative to domestic gas boiler heating systems in the South of Italy. Energy. 2019;173:59-74.
28. Ehyaei MA, Ahmadi A, El Haj Assad M, Rosen MA. Investigation of an integrated system combining an Organic Rankine Cycle and absorption chiller driven by geothermal energy: Energy, exergy, and economic analyses and optimization. Journal of Cleaner Production. 2020;258:120780.
29. Wei D, Zhang L, Alotaibi AA, Fang J, Alshahri AH, Almitani KH. Transient simulation and comparative assessment of a hydrogen production and storage system with solar and wind energy using TRNSYS. International Journal of Hydrogen Energy. 2022.
30. Kichou S, Markvart T, Wolf P, Silvestre S, Chouder A. A simple and effective methodology for sizing electrical energy storage (EES) systems based on energy balance. Journal of Energy Storage. 2022;49:104085.